



Brazilian Journal of Physics

ISSN: 0103-9733

luizno.bjp@gmail.com

Sociedade Brasileira de Física

Brasil

Jyoti Hazarika, Bhaskar; Choudhury, D. K.

Bounds on the Slope and Curvature of Isgur-Wise Function in a QCD-Inspired Quark Model

Brazilian Journal of Physics, vol. 41, núm. 2-3, septiembre, 2011, pp. 159-166

Sociedade Brasileira de Física

São Paulo, Brasil

Available in: <http://www.redalyc.org/articulo.oa?id=46421602011>

- How to cite
- Complete issue
- More information about this article
- Journal's homepage in redalyc.org

redalyc.org

Scientific Information System

Network of Scientific Journals from Latin America, the Caribbean, Spain and Portugal

Non-profit academic project, developed under the open access initiative

# Bounds on the Slope and Curvature of Isgur-Wise Function in a QCD-Inspired Quark Model

Bhaskar Jyoti Hazarika · D. K. Choudhury

Received: 22 February 2011 / Published online: 17 May 2011  
© Sociedade Brasileira de Física 2011

**Abstract** The quantum chromodynamics-inspired potential model pursued by us earlier has been recently modified to incorporate an additional factor ‘ $c$ ’ in the linear cum Coulomb potential. While it facilitates the inclusion of standard confinement parameter  $b = 0.183 \text{ GeV}^2$  unlike in previous work, it still falls short of explaining the Isgur-Wise function for the  $B$  mesons without ad hoc adjustment of the strong coupling constant. In this work, we determine the factor ‘ $c$ ’ from the experimental values of decay constants and masses and show that the reality constraint on ‘ $c$ ’ yields bounds on the strong coupling constant as well as on slope and curvature of Isgur-Wise function allowing more flexibility to the model.

**Keywords** Dalgarno method · Isgur-Wise function · Slope · Curvature · Nonrelativistic quark model · Potential models

**PACS** 12.39.-x · 12.39.Jh · 12.39.Pn

## 1 Introduction

In recent years, considerable experimental and theoretical efforts have been undertaken to understand the

physics of hadrons containing a heavy quark [1]. The Isgur-Wise (I-W) function [2] is an important quantity in this area of hadron physics. It is in this spirit that this function has been studied in various quark models [3–12] besides quantum chromodynamics (QCD) sum rule approach [13], the MIT bag model [14] and the Skyrme model [15].

Since one of the basic ingredients of the I-W function is the hadron wavefunction involving heavy quark [3–12], it is therefore meaningful to test any specific QCD-inspired quark model by calculating the I-W function and studying it phenomenologically. Sometimes back, a specific QCD-inspired quark model was proposed by us [16] which had later been used to calculate the I-W function as well [17–19].

One of the drawback of the model is that significant confinement effects could not be accommodated in the model [16–18] due to perturbative constraints coming from using the Dalgarno’s method [20]. Only recently [19], the standard confinement effect  $b = 0.183 \text{ GeV}^2$  [21] was accommodated in the improved version of QCD-inspired quark model, brought through the introduction of parameter ‘ $c$ ’ in the potential:  $V = \frac{-4\alpha_s}{3r} + br + c$  taking  $c \sim 1 \text{ GeV}$  as its natural scale and fixing  $A_0 = 1$ , where  $A_0$  is an undetermined factor appearing in the series solution of the Schrödinger equation ((8) of [19]). In earlier work [16–18], the unknown coefficient  $cA_0$  occurred in the wavefunction was set to zero.

One of the drawback of work [19] was the ad hoc enhancement of strong coupling constant needed to take into account of the slope and curvature of  $B$ ,  $B_s$  and  $B_c$  mesons. Also, the scaling of  $c \sim 1 \text{ GeV}$  as natural is questionable.

In this work, we take an alternative strategy to remove this ad hoc enhancement as well as the scaling

---

B. J. Hazarika (✉)  
Department of Physics, Pandu College,  
Guwahati 781012, India  
e-mail: bjh\_06@rediffmail.com

D. K. Choudhury  
Department of Physics, Gauhati University,  
Guwahati 781014, India

of  $c$ . We use the wavefunction at the origin (WFO) involving the unknown coefficient  $cA_0$  and fix it from the experimental values of masses and decay constants directly. The reality constraint on  $cA_0$  will be seen to yield lower bounds on the strong coupling constant  $\alpha_s$ , which would lead to the upper bounds on the slope and curvature of the I-W function.

The rest of the paper is organised as follows: Section 2 contains the formalism of the improved QCD-inspired quark model, Section 3 encloses the results and in Section 4 we draw conclusion and remarks.

## 2 Formalism

### 2.1 The Wavefunction

The spin-independent Fermi–Breit Hamiltonian for ground state ( $l = 0$ ), neglecting the contact term proportional to  $\delta^3$ , is [16, 17]:

$$H = H_0 + H',$$

$$= -\frac{\nabla^2}{2\mu} - \frac{4\alpha_s}{3r} + br + c. \quad (1)$$

where  $\alpha_s$  is the running coupling constant,  $b$  is the confinement parameter and  $c$  is another parameter whose significance will be cleared later.

As our objective is to look for the improvement over the earlier work [19], so in this work also we retain the same choice of  $\alpha_s$  values taken from the V-scheme [18, 26, 27] and  $b = 0.183 \text{ GeV}^2$  [19, 21] to investigate whether this approach leads to better results or not. With  $H_0 = -\frac{\nabla^2}{2\mu} - \frac{4\alpha_s}{3r}$  as the parent Hamiltonian and  $H' = br + c$  as the perturbed Hamiltonian, we obtain a ground state wavefunction up to the first-order correction using the Dalgarno method [20] of stationary state perturbation theory as:

$$\psi_{\text{conf}}(r) = N \left( cA_0 + \frac{1}{\sqrt{\pi a_0^3}} - \frac{\mu b a_0 r^2}{\sqrt{\pi a_0^3}} \right) e^{-\frac{r}{a_0}}. \quad (2)$$

where  $A_0$  is the unknown coefficient appearing in the series solution of the Dalgarno method.

Including the relativistic effect [22, 23], the wavefunction is:

$$\psi_{\text{conf+rel}}(r)$$

$$= N' \left( cA_0 + \frac{1}{\sqrt{\pi a_0^3}} - \frac{\mu b a_0 r^2}{\sqrt{\pi a_0^3}} \right) \left( \frac{r}{a_0} \right)^{-\epsilon} e^{-\frac{r}{a_0}}, \quad (3)$$

Here  $a_0$  is given by:

$$a_0 = \frac{3}{4\mu\alpha_s}, \quad (4)$$

and

$$\epsilon = 1 - \sqrt{1 - \frac{4\alpha_s}{3}}, \quad (5)$$

$N$  and  $N'$  are the normalization constants given by:

$$N^2 = \frac{1}{1 + \frac{45\mu^2 b^2 a_0^6}{8} - 3\mu b a_0^3 + \pi a_0^3 c^2 A_0^2 + \frac{2c A_0 \pi a_0^3}{\sqrt{\pi a_0^3}} - \frac{3\pi a_0^6 c A_0 \mu b}{\sqrt{\pi a_0^3}}}, \quad (6)$$

and

$$N'^2 = \frac{2^{7-2\epsilon}}{\Gamma(3-2\epsilon) X_1}. \quad (7)$$

where  $X_1$  is given in “Appendix”.

We note that the (2), (3), (6) and (7) are obtained from (4), (5), (6) and (7) of [19] exhibiting explicit dependence of  $cA_0$  in them.

### 2.2 Fixing of the Coefficient $cA_0$

The WFO is related to the decay constant  $f_p$  and the mass of the pseudoscalar meson  $M_p$  through the relation [16, 24]:

$$|\psi(0)|^2 = \frac{f_p^2 M_p}{12}. \quad (8)$$

Again from (2), we have:

$$|\psi(0)|^2 = N^2 \left[ c^2 A_0^2 + \frac{1}{\pi a_0^3} + \frac{2c A_0}{\sqrt{\pi a_0^3}} \right]. \quad (9)$$

Using (6) and (9), we arrive at the quadratic equation for  $cA_0$ :

$$A' (cA_0)^2 + B' (cA_0) + C' = 0, \quad (10)$$

where

$$A' = \pi a_0^3 |\psi(0)|^2 - 1, \quad (11)$$

$$B' = 2\sqrt{\pi a_0^3} |\psi(0)|^2 - 3\mu b a_0^3 \sqrt{\pi a_0^3} |\psi(0)|^2, \quad (12)$$

and

$$C' = |\psi(0)|^2 \left[ 1 + \frac{45\mu^2 b^2 a_0^6}{8} - 3\mu b a_0^3 \right] - \frac{1}{\pi a_0^3}. \quad (13)$$

Using the experimental values of  $f_p$  and  $M_p$  [25], we determine  $|\psi(0)|^2$  from (8) which in turn will yield two solutions for  $cA_0$  in (10):

$$cA_0 = \frac{-B' \pm \sqrt{B'^2 - 4A'C'}}{2A'}, \quad (14)$$

which will depend on  $\mu$ ,  $M_p$ ,  $f_p$  and  $\alpha_s$ . The solution corresponding to the +ve(−ve) sign of (14) will be termed as +ve(−ve) solution hereafter. It will be shown numerically that for a given  $\mu$ ,  $M_p$ , and  $f_p$ ,  $\alpha_s$  reaches the minimum value when the following condition is satisfied:

$$B'^2 - 4A'C' = 0. \quad (15)$$

The formalism involving (5)–(15) is strictly valid only without relativistic effect as the wavefunction at the origin with such effect (3) is not well-defined due to its singularity at the origin. For a subsequent analysis, we assume that  $cA_0$  does not deviate significantly from its non-relativistic value so that it can be used to calculate the slope and curvature of the I-W function even without relativistic effect.

### 2.3 Charge Radius (Slope) and Convexity Parameter (Curvature) of I-W Function

The Isgur-Wise function is written as [2, 17]:

$$\begin{aligned} \xi(v_\mu \cdot v'_\mu) &= \xi(y) \\ &= 1 - \rho^2(y-1) + C(y-1)^2 + \dots, \end{aligned} \quad (16)$$

$$\rho_{\text{conf}}^2 = \frac{\mu^2 \left[ 24\pi c^2 A_0^2 a_0^5 + 24a_0^2 + 630\mu^2 b^2 a_0^8 + 48cA_0 \sqrt{\pi a_0^7} - 180cA_0 \mu b \sqrt{\pi a_0^{13}} - 180\mu b a_0^5 \right]}{8\pi c^2 A_0^2 a_0^3 + 8 + 45\mu^2 b^2 a_0^6 + 16cA_0 \sqrt{\pi a_0^3} - 24\mu b c A_0 \sqrt{\pi a_0^3} - 24\mu b a_0^3}, \quad (22)$$

and:

$$C_{\text{conf}} = \frac{\mu^4 \left[ 60\pi c^2 A_0^2 a_0^7 + 60a_0^4 + 4725\mu^2 b^2 a_0^{10} + 120cA_0 \sqrt{\pi a_0^{10}} - 840cA_0 \mu b \sqrt{\pi a_0^{17}} - 840\mu b a_0^7 \right]}{16\pi c^2 A_0^2 a_0^3 + 16 + 90\mu^2 b^2 a_0^6 + 32cA_0 \sqrt{\pi a_0^3} - 48\mu b c A_0 \sqrt{\pi a_0^3} - 48\mu b a_0^3}. \quad (23)$$

With the wavefunction (3) in (20), i.e. including both relativistic and confinement effect, the charge radius  $\rho_{\text{conf+rel}}^2$  and convexity parameter  $C_{\text{conf+rel}}$  are given by:

$$\rho_{\text{conf+rel}}^2 = \frac{\mu^2 a_0^2 (4 - 2\epsilon) (3 - 2\epsilon) [X_1]}{4[X_2]}, \quad (24)$$

where

$$y = v_\mu \cdot v'_\mu, \quad (17)$$

and  $v_\mu$  and  $v'_\mu$  being the four velocity of the heavy meson before and after the decay. The quantity  $\rho^2$  is the slope of I-W function at  $y = 1$  and known as charge radius:

$$\rho^2 = \frac{\partial \xi}{\partial y} \Big|_{y=1}, \quad (18)$$

The second-order derivative is the curvature of the I-W function known as convexity parameter:

$$C = \frac{1}{2} \left[ \frac{\partial^2 \xi}{\partial^2 y} \Big|_{y=1} \right]. \quad (19)$$

For the heavy-light flavor mesons, the I-W function can also be written as [6, 17]:

$$\xi(y) = \int_0^{+\infty} 4\pi r^2 |\psi(r)|^2 \cos pr dr, \quad (20)$$

where

$$p^2 = 2\mu^2(y-1). \quad (21)$$

Equation (20) holds good for both relativistic and non-relativistic case. The wavefunction  $\psi(r)$  takes different form for both the cases. Without relativistic effect, it is given by (2) and with relativistic effect it is given by (3).

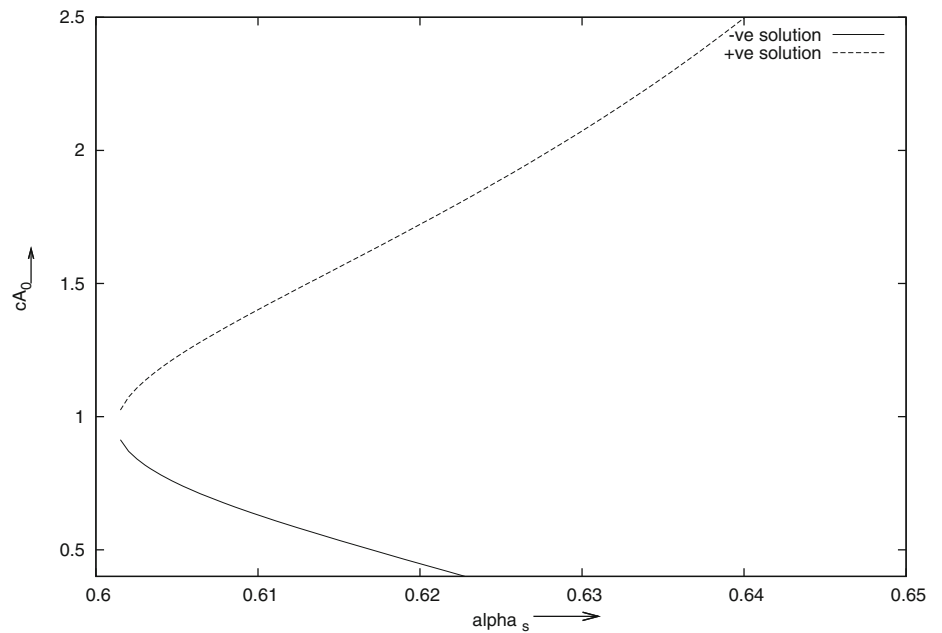
With the wavefunction (2) in (20), i.e. including confinement, only the charge radius  $\rho_{\text{conf}}^2$  and convexity parameter  $C_{\text{conf}}$  are, respectively, given by:

and

$$C_{\text{conf+rel}} = \frac{\mu^4 a_0^4 (6 - 2\epsilon) (5 - 2\epsilon) (4 - 2\epsilon) (3 - 2\epsilon) [X_3]}{96[X_2]}. \quad (25)$$

where  $X_1$ ,  $X_2$  and  $X_3$  are given in “Appendix”.

**Fig. 1** Variation of  $cA_0$  vs  $\alpha_s$  for  $D$  meson. The +ve(–ve) solution of (14) corresponds to the dashed (solid) line and the two lines nearly coincide at  $\alpha_s \sim 0.601$ , the lower bound on  $\alpha_s$  corresponding to the solution of (15) for  $D$  meson



We note that (24) and (25) are equivalent to (18) and (19) of [19] exhibiting explicit  $cA_0$  dependence.

### 3 Results

#### 3.1 Values of $cA_0$ and Lower Bounds on $\alpha_s$

As noted earlier,  $cA_0$  depends on  $\mu$ ,  $M_p$ ,  $f_p$  and  $\alpha_s$ . In Fig. 1, 2, 3, 4 and 5, we plot  $cA_0$  vs  $\alpha_s$  for  $D$ ,  $D_s$ ,

$B$ ,  $B_s$  and  $B_c$  mesons. It shows that  $\alpha_s$  tends to reach the minimum value when two solutions of (14) almost merge satisfying the condition (15). This feature is true for any set of the parameters  $\mu$ ,  $f_p$  and  $M_p$ . In Table 1, we give the lower bounds on  $\alpha_s$  for mesons having  $c$  and  $b$  quarks.

The dependence of  $cA_0$  on  $\alpha_s$  and  $\mu$  can be noted as follows: With constant  $\mu$ ,  $cA_0$  decreases with  $\alpha_s$  values rising and vice versa. On the other hand, with constant

**Fig. 2** Variation of  $cA_0$  vs  $\alpha_s$  for  $B$  meson. The +ve(–ve) solution of (14) corresponds to the dashed (solid) line and the two lines nearly coincide at  $\alpha_s \sim 0.652$ , the lower bound on  $\alpha_s$  corresponding to the solution of (15) for  $B$  meson

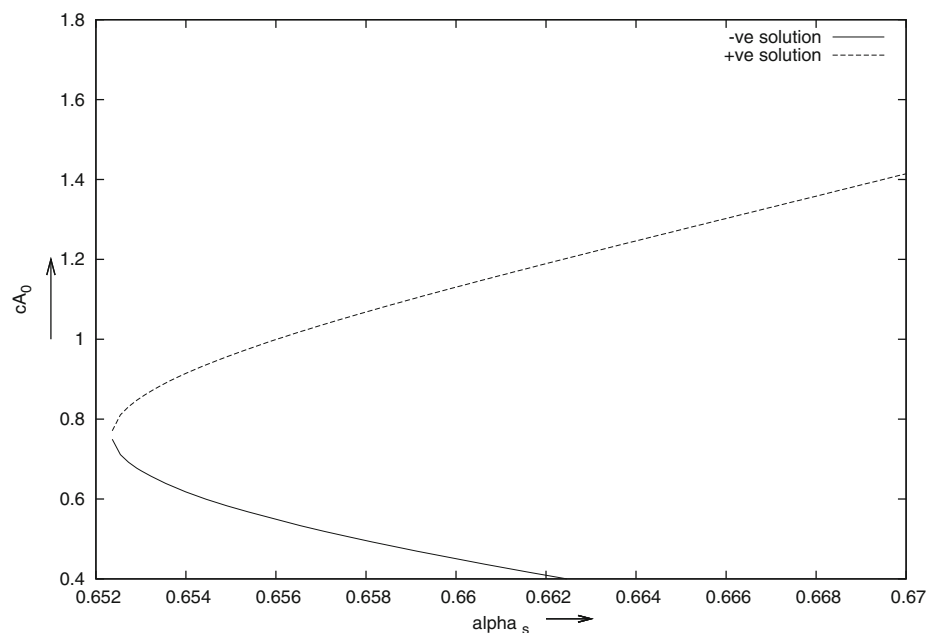
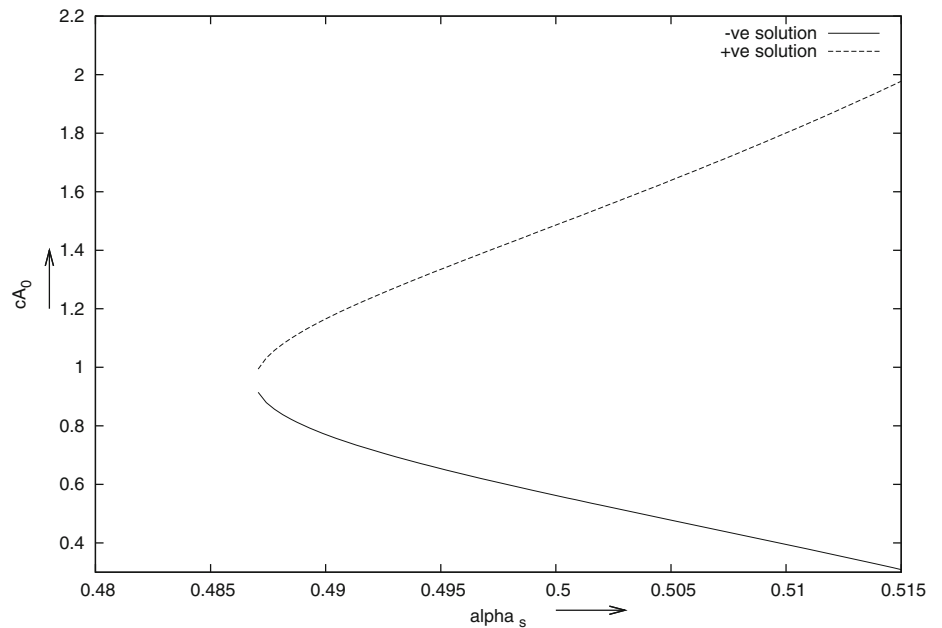


**Fig. 3** Variation of  $cA_0$  vs  $\alpha_s$  for  $D_s$  meson. The +ve(–ve) solution of (14) corresponds to the dashed (solid) line and the two lines nearly coincide at  $\alpha_s \sim 0.49$ , the lower bound on  $\alpha_s$  corresponding to the solution of (15) for  $D_s$  meson



$\alpha_s$ ,  $cA_0$  increases (decreases) with increase (decrease) in  $\mu$ .

### 3.2 Bounds on Slope and Curvature of the I-W Function

Using the lower bounds on  $\alpha_s$  for each heavy–light and heavy–heavy mesons, we obtain upper bounds on the

slope and curvature of the I-W function using (23), (24), (25) and (26). They are listed in Table 2. We note that with increasing  $\alpha_s$  values, the slope and curvature decrease and henceforth the lower bound on  $\alpha_s$  corresponds to the upper bound on  $\rho^2$  and  $C$ .

In Table 3, we record the predictions of the slope and curvature of the I-W function in various models while in Table 4, we reproduce the corresponding predictions of the model of [19] with  $c = 1$  GeV and  $A_0 = 1$  in

**Fig. 4** Variation of  $cA_0$  vs  $\alpha_s$  for  $B_s$  meson. The +ve(–ve) solution of (14) corresponds to the dashed (solid) line and the two lines nearly coincide at  $\alpha_s \sim 0.493$ , the lower bound on  $\alpha_s$  corresponding to the solution of (15) for  $B_s$  Meson

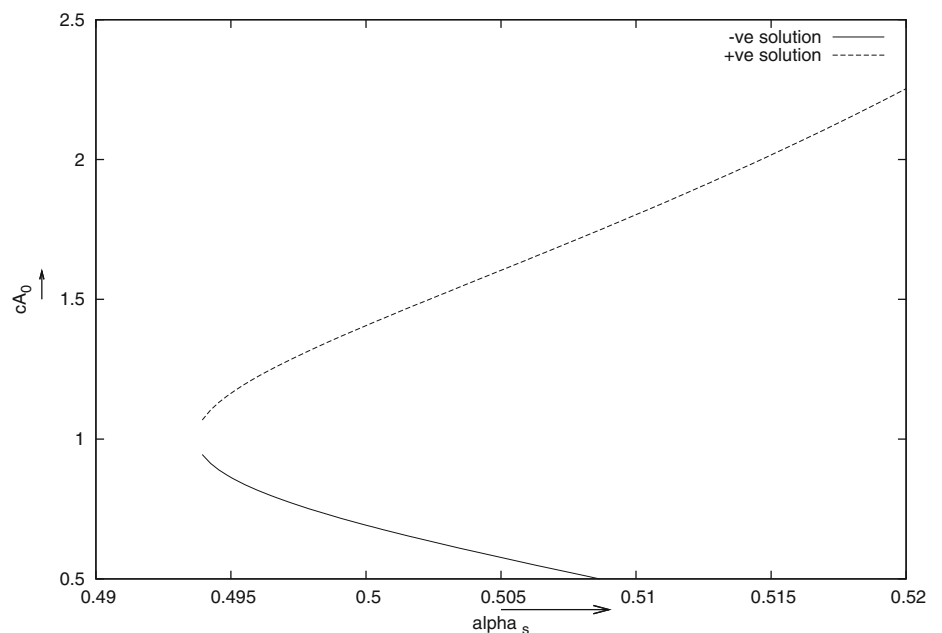


**Fig. 5** Variation of  $cA_0$  vs  $\alpha_s$  for  $B_c$  Meson. The +ve(−ve) solution of (14) corresponds to the dashed (solid) line and the two lines nearly coincide at  $\alpha_s \sim 0.302$ , the lower bound on  $\alpha_s$  corresponding to the solution of (15) for  $B_c$  meson

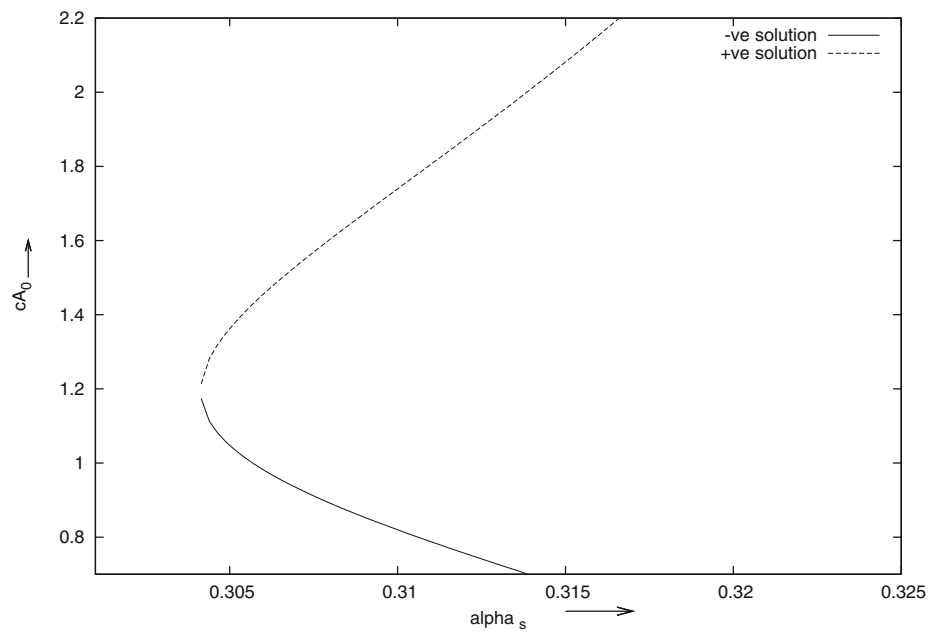


**Table 1** Lower bounds on  $\alpha_s$

Mesons	Quark content	$\mu$ (GeV) [25]	$M_p$ (GeV) [25]	$f_p$ (GeV) [25]	$cA_0$	Lower bound on $\alpha_s$
$D$	$c\bar{u}/c\bar{d}$	0.276	1.869	0.192	0.9665	$\sim 0.601$
$B$	$\bar{b}u/\bar{b}d$	0.315	5.279	0.210	0.7653	$\sim 0.652$
$D_s$	$c\bar{s}$	0.368	1.968	0.157	0.9543	$\sim 0.49$
$B_s$	$\bar{b}s$	0.44	5.279	0.171	0.999	$\sim 0.493$
$B_c$	$\bar{b}c$	1.18	5.37	0.36	1.167	$\sim 0.302$

**Table 2** Upper bounds on slope and curvature

Meson (quark content)	Slope $\rho^2$		Curvature $C$	
	Without relativistic effect	With relativistic effect	Without relativistic effect	With relativistic effect
$D(c\bar{u}/c\bar{d})$	6.78	1.675	13.19	5.138
$B(\bar{b}u/\bar{b}d)$	5.78	1.016	9.58	1.29
$D_s(c\bar{s})$	9.115	3.067	26.48	14.32
$B_s(\bar{b}s)$	11.92	2.652	34.49	6.902
$B_c(\bar{b}c)$	28.46	10.39	219.46	45.23

**Table 3** Predictions of the slope and curvature of the I-W function in various models

Model	Value of $\rho^2$	Value of curvature $C$
Yaouanc et al. [28]	$\geq 0.75$	..
Yaouanc et al. [12]	$\geq 0.75$	$\geq 0.47$
Rosner et al. [29]	1.66	2.76
Mannel et al. [30, 31]	0.98	0.98
Pole Ansatz [32]	1.42	2.71
MIT bag model [14]	2.35	3.95
Simple quark model [3]	1	1.11
Skryme model [15]	1.3	0.85
QCD sum rule [13]	0.65	0.47
Relativistic three quark model [4]	1.35	1.75
Infinite momentum frame quark model [5]	3.04	6.81

**Table 4** Predictions of the slope and curvature of the I-W function in the QCD inspired quark model according to [19] with  $c = 1$  and  $A_0 = 1$  taking relativistic and confinement effect in V-scheme

Meson	$\alpha_s$	Slope ( $\rho^2$ )	Curvature( $C$ )
$D$	0.625	1.136	5.377
$D_s$	0.625	1.083	3.583
$B$	(a)0.261	(a)128.128	(a)5212
	(b)0.60	(b)1.329	(b)7.2
$B_s$	(a)0.261	(a)112.759	(a)4841
	(b)0.60	(b)1.257	(b)4.379
$B_c$	(a)0.261	(a)44.479	(a)2318
	(b)0.60	(b)1.523	(b)0.432

This table is nothing but a replica of the last rows of Tables 1, 2 and 3 of [19]

V-scheme [26, 27] for various mesons. Two set of values for  $B$ ,  $B_s$  and  $B_c$  mesons are shown in the table where case (a) represents the actual values for  $\rho^2$  and  $C$  in that work with  $\alpha_s = 0.261$ , while case (b) represents those for an ad hoc adjustable value of  $\alpha_s = 0.60$  in order to show the usefulness of large  $\alpha_s$  as mentioned in [19]. The  $\alpha_s$  values were already large for  $D$  and  $D_s$  mesons, so no ad hoc adjustment was necessary that might lead to two set of values.

#### 4 Conclusion and Remarks

We have shown that the reality bound on  $cA_0$  puts a lower limit on  $\alpha_s$  and a corresponding upper limit on  $\rho^2$  and  $C$ . Furthermore, with  $cA_0$ , that the upper bounds on  $\rho^2$  and  $C$  decrease, which is evident from the above list of bounds (Table 2). The estimated upper bounds on  $\rho^2$  and  $C$  for all the mesons are found to be consistent with other models and data (Table 3) without making any ad hoc enhancement of the strong coupling constant as had been done in [19] (Table 4). From the phenomenological point of view, we note that in the nonrelativistic limit, the universal form factor and Isgur-Wise function for semileptonic decay  $B \rightarrow D^*lv$  are identical when subleading terms in velocity and terms of order  $O\left(\frac{E_b}{m_Q}\right)$  are neglected with  $E_b$  as the binding energy and  $m_Q$  as the mass of heavy quark [33]. However, even if we make calculation for the universal form factor for finite mass, we obtain to first order in  $(y-1)$  as  $0.8-2.57(y-1)$  which seems to be satisfactory [33, 34].

It is worth notable that in the limit  $cA_0 \rightarrow 0$ , there will be no bounds on  $\alpha_s$  as well as on  $\rho^2$  and  $C$ ; rather, fixed values of  $\alpha_s$  have to be used to get definite set of  $\rho^2$  and  $C$ . So, in that case, the analysis will turn to that of [17, 18] where large confinement could not be (i.e.

$b = 0.183 \text{ GeV}^2$ ) incorporated, e.g. Tables 1 and 3 of [17] and Tables 2 and 3 of [18].

We conclude this paper with a comment on the physical significance of the factor ‘ $c$ ’ that has become so crucial for our analysis of bounds on slope and curvature. It is common wisdom that a constant potential like ‘ $c$ ’ just scales the energies and does not affect the wavefunction nor does it change physics. This can be seen from the hydrogen atom problem with the potential  $V(r) = -\frac{A}{r} + c$ . However, if one uses ‘ $c$ ’ as the perturbation instead of as parent in the Dalgarno method of perturbation theory [20], the normalized wavefunction for the  $H$ -atom becomes

$$\psi(r) = \left[ \frac{1}{1 + \pi a_0^3 c^2 A_0^2 + \frac{2cA_0\pi a_0^3}{\sqrt{\pi a_0^3}}} \right] \left( cA_0 + \frac{1}{\sqrt{\pi a_0^3}} \right) e^{-\frac{r}{a_0}},$$

which is to be compared with the normalized wavefunction with ‘ $c$ ’ as parent:

$$\psi(r) = \left( \frac{1}{\sqrt{\pi a_0^3}} \right) e^{-\frac{r}{a_0}}.$$

Thus, the perturbative child ‘ $c$ ’ rather than the parent ‘ $c$ ’ plays the crucial role in the present analysis.

#### Appendix

$X_1$ ,  $X_2$  and  $X_3$  are evaluated as

$$\begin{aligned} X_1 = & 64\pi c^2 A_0^2 a_0^3 + 64 + \mu^2 b^2 a_0^6 \\ & \times (8 - 2\epsilon)(7 - 2\epsilon)(6 - 2\epsilon)(5 - 2\epsilon) \\ & + 128cA_0\sqrt{\pi a_0^3} - 16cA_0\mu b\sqrt{\pi a_0^9}(6 - 2\epsilon)(5 - 2\epsilon) \\ & - 16\mu b a_0^3(6 - 2\epsilon)(5 - 2\epsilon), \end{aligned} \quad (26)$$

$$\begin{aligned} X_2 = & 64\pi c^2 A_0^2 a_0^3 + 64 + \mu^2 b^2 a_0^6 \\ & \times (6 - 2\epsilon)(5 - 2\epsilon)(4 - 2\epsilon)(3 - 2\epsilon) \\ & + 128cA_0\sqrt{\pi a_0^3} - 16cA_0\mu b\sqrt{\pi a_0^9}(4 - 2\epsilon)(3 - 2\epsilon) \\ & - 16\mu b a_0^3(4 - 2\epsilon)(3 - 2\epsilon), \end{aligned} \quad (27)$$

and

$$\begin{aligned} X_3 = & 64\pi c^2 A_0^2 a_0^3 + 64 + \mu^2 b^2 a_0^6 \\ & \times (10 - 2\epsilon)(9 - 2\epsilon)(8 - 2\epsilon)(7 - 2\epsilon) \\ & + 128cA_0\sqrt{\pi a_0^3} - 16cA_0\mu b\sqrt{\pi a_0^9}(8 - 2\epsilon)(7 - 2\epsilon) \\ & - 16\mu b a_0^3(8 - 2\epsilon)(7 - 2\epsilon). \end{aligned} \quad (28)$$



Not only the above expressions but also all the integrals in the analysis are evaluated with the help of Gamma function, given by:

$$\frac{\Gamma(n+1)}{\alpha^{n+1}} = \int_0^{+\infty} r^n e^{-\alpha r} dr. \quad (29)$$

## References

1. M. Neubert, Phys. Rep. **245**, 259 (1994)
2. N. Isgur, M.B. Wise, Phys. Lett. B **232**, 113 (1989)
3. B. Holdom, M. Sutherland, J. Mureika, Phys. Rev. D **49**, 2359 (1994)
4. M.A. Ivanov, V.E. Lyubovitskij, L.G. Körner, P. Kroll, Phys. Rev. D **56**, 348 (1997)
5. B. König, J.G. Körner, M. Krämer, P. Kroll, Phys. Rev. **56**, 4282 (1997)
6. F.E. Close, A. Wambach, Nucl. Phys. B **412**, 169 (1994)
7. H.W. Huang, Phys. Rev. D **56**, 1579 (1979)
8. D. Melikhov, Phys. Rev. D **53**, 2460 (1996)
9. M.R. Ahmady, R.R. Mendel, J.D. Talman, Phys. Rev. D **52**, 254 (1995)
10. M.G. Olsson, S. Veseli, Fermilab-Pub-96/418-T (1997)
11. M.G. Olsson, S. Veseli, Phys. Rev. D **51**, 2224 (1995)
12. A. Le Yaouanc, L. Oliver, J.C. Raynal, Phys. Rev. D **69**, 094022 (2004)
13. Y.B. Dai, C.S. Huang, M.Q. Huang, C. Liu, Phys. Lett. B **387**, 379 (1996)
14. M. Sadzikowski, K. Zalewski, Z. Phys. C **59**, 667 (1993)
15. E. Jenkins, A. Manohar, M.B. Wise, Nucl. Phys. B **396**, 38 (1996)
16. D.K. Choudhury, P. Das, D.D. Goswami, J.N. Sharma, Pramana J. Phys. **44**, 519 (1995)
17. D.K. Choudhury, N.S. Bordoloi, IJMPA **15**(23), 3667 (2000)
18. D.K. Choudhury, N.S. Bordoloi, MPLA **17**(29), 1909 (2002)
19. D.K. Choudhury, N.S. Bordoloi, MPLA **24**(6), 443 (2009)
20. A. Ghatak, S. Lokanathan, in *Quantum Mechanics* (McGraw Hill, New York, 1997), p. 291
21. E. Eichten, Phys. Rev. D **17**, 3090 (1978)
22. J.J. Sakurai, in *Advanced Quantum Mechanics* (Addison-Wesley, Boston, 1986), p. 128
23. C. Itzykson, J. Zuber, in *Quantum Field Theory*, (International Student Edition, McGraw Hill, Singapore, 1986), p. 79
24. V.O. Galkin, A. Yu Mishurov, R.N. Faustov, Sov. J. Nucl. Phys. **53**, 1026 (1991)
25. D.E. Groom et al., Particle Data Group. Eur. Phys. J. C **15**, 1 (2000)
26. Y. Schröder, Phys. Lett. B **447**, 321 (1999)
27. Y. Schröder, Nucl. Phys. Proc. Suppl. **86**, 525 (2000)
28. A. Le Yaouanc, L. Oliver, O. Pene, J.C. Raynal, Phys. Lett. B **365**, 319 (1996)
29. J.L. Rosner, Phys. Rev. D **44**, 3732 (1990)
30. T. Mannel, W. Roberts, Z. Ryzak, Phys. Rev. D **44**, R18 (1991)
31. T. Mannel, W. Roberts, Z. Ryzak, Phys. Lett. B **255**, 593 (1993)
32. M. Neubert, Phys. Lett. B **264**, 455 (1991)
33. F. Jugeau, A. Le Yaouanc, L. Oliver, J.C. Raynal; Phys. Rev. D **70**, 114020 (2004)
34. F.E. Close, A. Wambach, RAL-94-041, OUTP-94 09P (1994)